NACA

RESEARCH MEMORANDUM

A FLIGHT-TEST STUDY OF TOTAL-PRESSURE DISTORTION

IN A THICK-LIPPED NOSE INLET

By Rodney C. Wingrove

Ames Aeronautical Laboratory
Moffett Field, Calif.

This material contains information affecting the National Defense of the United States within the meaning of the espionage laws, Title 18, U.S.C., Secs. 793 and 794, the transmission or revelation of which in any manner to an unauthorized person is prohibited by law.

NATIONAL ADVISORY COMMITTEE
FOR AERONAUTICS
WASHINGTON
June 30, 1958

NACA RM A58B07

NATIONAL ADVISORY COMMITTEE FOR AERONAUTICS

RESEARCH MEMORANDUM

A FLIGHT-TEST STUDY OF TOTAL-PRESSURE DISTORTION

IN A THICK-LIPPED NOSE INLET

By Rodney C. Wingrove

SUMMARY

Flight tests were conducted on a thick-lipped nose inlet of a transonic swept-wing aircraft. No engine operating problems have been encountered with this airplane and, therefore, it is felt that total-pressure distortions measured for this inlet should provide a basis for comparison in the evaluation of other inlet types.

The total-pressure recovery and distortion at the compressor face were measured over the maneuvering range of the airplane for Mach numbers up to 1.03. The maximum distortion in the point measurements of total pressure was 8 percent. A maximum radial distortion of 5 percent and a circumferential distortion of 2.5 percent were measured. Variation in angle of attack up to 16° had negligible effect on the total-pressure recovery and distortion.

INTRODUCTION

Recent investigations (refs. 1 and 2) have indicated that distortion of the air flow at the face of the compressor of a turbojet engine results in performance losses and increases the danger of stalling the compressor. New high-speed aircraft are incorporating complex forms of inlet geometry which increase the possibility of flow distortion and therefore are more susceptible to performance losses and compressor stall (see ref. 3).

To establish a basis for comparison in the evaluation of the internal flow characteristics on more advanced inlet types, the characteristics of a satisfactory thick-lipped inlet have been investigated and are presented herein. Since the function of an inlet is to supply air to the turbojet engine with a high recovery and a minimum of distortion, this investigation included both the total-pressure recovery and distortion characteristics of the inlet. Flight tests were conducted over the Mach number range from 0.3 to 1.03. The angle-of-attack range was 1° to 16° at the lower Mach numbers but was more limited at the higher Mach numbers.

NOTATION

The following symbols and subscripts are used in this report. A general discussion of these inlet terms is available in reference 4.

A   area, sq ft

h_p pressure altitude, ft

p_t total pressure, lb/sq ft

M_∞ flight Mach number

m   mass flow, ρAV, slugs/sec

$\dfrac{m_2}{m_\infty}$ mass-flow ratio, $\dfrac{\rho_2 A_2 V_2}{\rho_\infty A_2 V_\infty}$

T_t total temperature, °R

V   air velocity, ft/sec

W   air flow, lb/sec

$\dfrac{W\sqrt{\theta}}{\delta}$ corrected air flow, lb/sec

α angle of attack, deg

δ pressure ratio, $\dfrac{p_t}{2116}$

ρ mass density of air, slugs/cu ft

θ temperature ratio, $\dfrac{T_t}{519}$

Subscripts

c   circumferential

l local conditions at the face of the total-pressure rake (fig. 3)

r   radial

∞ free stream

1   capture area station of the inlet, station ①, area 550 sq in.

2   minimum area section of the inlet, station ②, area 350 sq in.

3   average conditions at the face of the compressor, station ③,
        area 440 sq in.

INSTRUMENTATION AND EQUIPMENT

Test Airplane

The swept-wing fighter airplane used for this investigation is shown
in figure 1. This airplane incorporates the nose-type inlet shown in
figure 2 mated to a J47-13 engine. Details and pertinent dimensions of
this inlet are shown in figure 3.

Instrumentation and Tests

The total-pressure measurements were obtained from four rakes, of
five total-pressure tubes each, mounted 14 inches ahead of the compressor
face as indicated in figure 3. Detailed dimensions of these rakes are
presented in figure 4 and a photograph of the probe installation is shown
in figure 5. The pressures were recorded by -350 to 1100 pounds per
square foot differential pressure cells located about 8 feet from the
rakes and the cells were referenced to the free-stream static-pressure
system. The estimated frequency response of the measuring system indi-
cates no appreciable phase shift up to approximately 15 cycles per second.
With this measuring apparatus no total-pressure fluctuation was noted.

Measurements were made under steady-state conditions; that is,
constant throttle settings and steady aircraft conditions. Standard
NACA recording instruments and recording oscillographs synchronized at
1/10-second intervals were used to record the test data. True Mach num-
ber was obtained from a nose-boom airspeed system by means of the cali-
bration described in reference 5. Angle of attack was measured by a
floating vane located on the nose boom 9 feet ahead of the nose of the
airplane. Corrections were made to the measured angle of attack for
boom deflection and vane floating angle. The corrected engine air flow
was obtained from the altitude wind-tunnel tests of reference 6 using
the pilot's indicated rpm and the free-air temperature recorded by a
weather balloon.

Accuracy

The estimated precision of the measurements based on the least count of the instruments and other contributing factors is:

Mach number	±0.01
Local pressure	±5 lb/sq ft
Angle of attack	±0.5°
Corrected air flow	±3 percent

RESULTS AND DISCUSSION

Radial Total-Pressure Profiles

Typical pressures measured by the total-pressure rakes located at the face of the compressor are shown in figure 6. Contour plots are presented in figure 7 to illustrate a few selected examples of pressure variations around half the duct. Regions of lowest pressure recovery are evident along the outer wall of the inlet especially at the higher inlet air flows and also near the top and bottom of the duct.

While the flow distortion will be emphasized in analyzing the data in this report, it is obvious that an air-induction system is not satisfactory if a uniform flow field is obtained at the expense of lowered pressure recovery. Thus flow distortion and recovery characteristics must be considered together.

Average Total-Pressure Recovery

The average pressure recovery at the compressor face was obtained by integrating the total pressure measured by each rake and using the mean value for each rake to obtain the arithmetic average total pressure for all the rakes. The pressure recovery is presented in figure 8 as a function of mass-flow ratio for a constant angle of attack near 3°.

Figure 9 presents the average pressure recovery as a function of angle of attack. The inlet was found to exhibit little change in characteristics with angle of attack, presumably because of the large leading-edge radius and the upper overhang. Data from reference 7 for a circular inlet having a comparably large leading-edge radius are shown in figures 9(a) and 9(b). The model tests indicate no pressure recovery change

up to 20° angle of attack at a mass-flow ratio of 1.8; but at a mass-flow ratio of 2.1 there is a loss of pressure recovery between 15° and 20° angle of attack caused by leading-edge separation. In the flight tests no leading-edge separation was apparent up to the 16° angle of attack attained. Over the complete maneuvering range of this airplane for Mach numbers up to 1.03, no effect of angle of attack on pressure recovery was noted.

<center>Total-Pressure Distortion</center>

The specific ways in which inlet flow distortion affects joint inlet-engine operation have not been clearly established. However, studies, such as references 2, 8, and 9, have been made to define a flow distortion index that takes account of important engine parameters as well as inlet flow distortion parameters; for example,

$$D' = f\left(\frac{\Delta p_t}{p_t}, \varphi, v, N, r, \text{etc.}\right)$$

where

D' flow-distortion index

$\dfrac{\Delta p_t}{p_t}$ total-pressure distortion

φ angular extent of circumferential distortion

v axial velocity at compressor

N engine rpm

r rotor blade size and location

It can be seen that only the first two variables, $\Delta p_t/p_t$ and φ, are primarily functions of the inlet shape, and the other variables are engine functions.

It is the purpose here to investigate the inlet variable $\Delta p_t/p_t$. The value φ has little significance in this investigation because of the inherently low circumferential distortion of this type of inlet. However, where large circumferential distortions occur, such as with side inlets or ducts with curvature, this parameter would be more significant.

The total-pressure distributions shown in figures 6 and 7 indicate both radial distortion (from the inner wall to the outer wall) and circumferential distortion (from the top of the inlet to the bottom of the inlet), as well as a maximum pressure difference from one point to another. In order to study these various forms of pressure distribution, the total-pressure distortion parameter has been calculated in the following three ways. A discussion of these distortion parameters is available in reference 10.

Point total-pressure distortion $\dfrac{p_{t_{l_{max}}} - p_{t_{l_{min}}}}{p_{t_3}}$

Average radial total-pressure distortion $\dfrac{\bar{p}_{t_{r_{max}}} - \bar{p}_{t_{r_{min}}}}{p_{t_3}}$

Average circumferential total-pressure distortion $\dfrac{\bar{p}_{t_{c_{max}}} - \bar{p}_{t_{c_{min}}}}{p_{t_3}}$

where

p_{t_3} average total pressure at station ③

p_{t_l} local total pressure measured by any of the 20 tubes (refer to fig. 4)

$\bar{p}_{t_r}$ average total pressure at any of the five radial locations

$\bar{p}_{t_c}$ average total pressure at any of the four circumferential positions

The total-pressure distortion measured during this flight investigation is shown in figure 10 as a function of the corrected inlet air flow. The total-pressure distortion increased with increases in air flow and the maximum distortion levels measured were 8-percent point distortion, 5-percent average radial distortion, and 2.5-percent average circumferential distortion.

The trend of increasing total-pressure distortion with increasing inlet air-flow rate has been explained in reference 11. In order to compare the total-pressure distortion of various inlet shapes it is best to compare the distortion levels with some standard. The standard used to compare these test results is the total-pressure distortion caused by the velocity profiles for fully developed turbulent flow in a smooth pipe. Figure 11 presents the curves of pipe-flow total-pressure distortion from reference 12 compared with these test results. The pipe-flow curves serve only as a guide for evaluating and comparing test results

and, because the magnitude of the pipe-flow curves is primarily a function of the radius used for comparison, the curves do not imply limits for test data. A comparison of the test results with the pipe-flow curves indicates that the point distortions for the tests were slightly higher while the average radial distortions were slightly lower than the pipe-flow values. The average circumferential distortion for pipe flow would be zero, but for an actual inlet it would depend primarily on duct geometry (i.e., bends, obstructions, etc.). The data of figure 11 indicate a very low level of circumferential distortion for this inlet. The general trend of the data with corrected air flow is the same as predicted from the fully developed pipe-flow curves.

The curves for fully developed turbulent flow in figure 11 indicate an effect of altitude on the distortion profile caused by the change in pipe friction drag with Reynolds number. Some of the flight test data in figure 10 show this effect of altitude, but generally the pressure measuring system is not accurate enough to detect this small difference.

Figure 12 shows the effect of Mach number on the total-pressure distortion. The total-pressure distortion tends to increase only slightly with increases in Mach number.

The effect of angle of attack on the total-pressure distortion is shown in figure 13. The results show the same trend as indicated by the average pressure recoveries - that there is a negligible effect of angle of attack for this inlet up to 16° angle of attack. Over the maximum maneuvering range of the airplane for Mach numbers up to 1.03 no distortion due to angle of attack was noted.

The amount of total-pressure distortion measured during these flight tests apparently had no effect on the engine operating characteristics. Over the range of variables encountered no tendency toward compressor stall or surge was noted.

SUMMARY OF RESULTS

A flight-test study was conducted on a thick-lipped nose inlet that presented no operating problems such as compressor stall or surge. The flight-test data obtained during steady-state maneuvers indicated:

1. Total-pressure distortions of 8 percent in point measurements, 5 percent in average radial measurements, and 2.5 percent in average circumferential measurements were the largest encountered.

2. Angles of attack up to 16° had negligible effect on either the average pressure recovery or total-pressure distortion.

3.   Increases in Mach number up to 1.0 resulted in small increases in total-pressure distortion.

Ames Aeronautical Laboratory
      National Advisory Committee for Aeronautics
            Moffett Field, Calif., Feb. 7, 1958

REFERENCES

1.   Conrad, E. William, Hanson, Morgan P., and McAulay, John E.:   Effect
       of Inlet-Air-Flow Distortion on Steady-State Altitude Performance
       of an Axial-Flow Turbojet Engine.   NACA RM E55A04, 1955.

2.   Sens, William H., Bailey, W. S., and Smith, C. B.:   Effects of
       Supersonic Inlet Characteristics on Gas Turbine Performance.   Pratt
       and Whitney Aircraft Inst. Rep. 471, May 19, 1955.

3.   Larson, Terry J., Thomas, George M., and Bellman, Donald R.:   The
       Induction System Characteristics and Engine Surge Occurrence for
       Two Fighter-Type Airplanes.   NACA RM H58C14, 1958.

4.   Davis, Wallace F., and Scherrer, Richard: Aerodynamic Principles for
       the Design of Jet-Engine Induction Systems.   NACA RM A55F16, 1956.

5.   Thompson, Jim Rogers, Bray, Richard S., and Cooper, George E.:
       Flight Calibration of Four Airspeed Systems on a Swept-Wing Air-
       plane at Mach Numbers up to 1.04 by the NACA Radar-Phototheodolite
       Method.   NACA TN 3526, 1955.   (Supersedes NACA RM A50H24)

6.   Conrad, E. William, and Sobolewski, Adam E.:   Altitude-Wind-Tunnel
       Investigation of J47 Turbojet-Engine Performance.   NACA RM E9G09,
       1949.

7.   Blackaby, James R.:   Low-Speed Investigation of the Effects of Angle
       of Attack on the Pressure Recovery of a Circular Nose Inlet With
       Several Lip Shapes.   NACA TN 3394, 1955.

8.   Steffens, Charles, Jr., and Throndson, L. W.:   Development of a
       Method for Correlating the Effect of Various Types of Circumferen-
       tial Inflow Distortion on the Stall Characteristics of Axial Flow
       Compressor Engines.   Pratt and Whitney Aircraft Inst. Rep. 480,
       Sept. 30, 1955.

9.   Alford, J. S.:   Inlet Duct-Engine Flow Compatibility.   Presented at
       the 5th International Aeronautical Conference, June 20-24, 1955.
       (Also IAS preprint 566)

10. Valentine, Harold H., and Beale, William T.: Experimental Investigation of Distortion Removal Characteristics of Several Free-Wheeling Fans. NACA RM E57I12, 1958.

11. Sterbentz, William H.: Factors Controlling Air-Inlet Flow Distortions. NACA RM E56A30, 1956.

12. Deissler, Robert G.: Analytical and Experimental Investigation of Adiabatic Turbulent Flow in Smooth Tubes. NACA TN 2138, 1950.
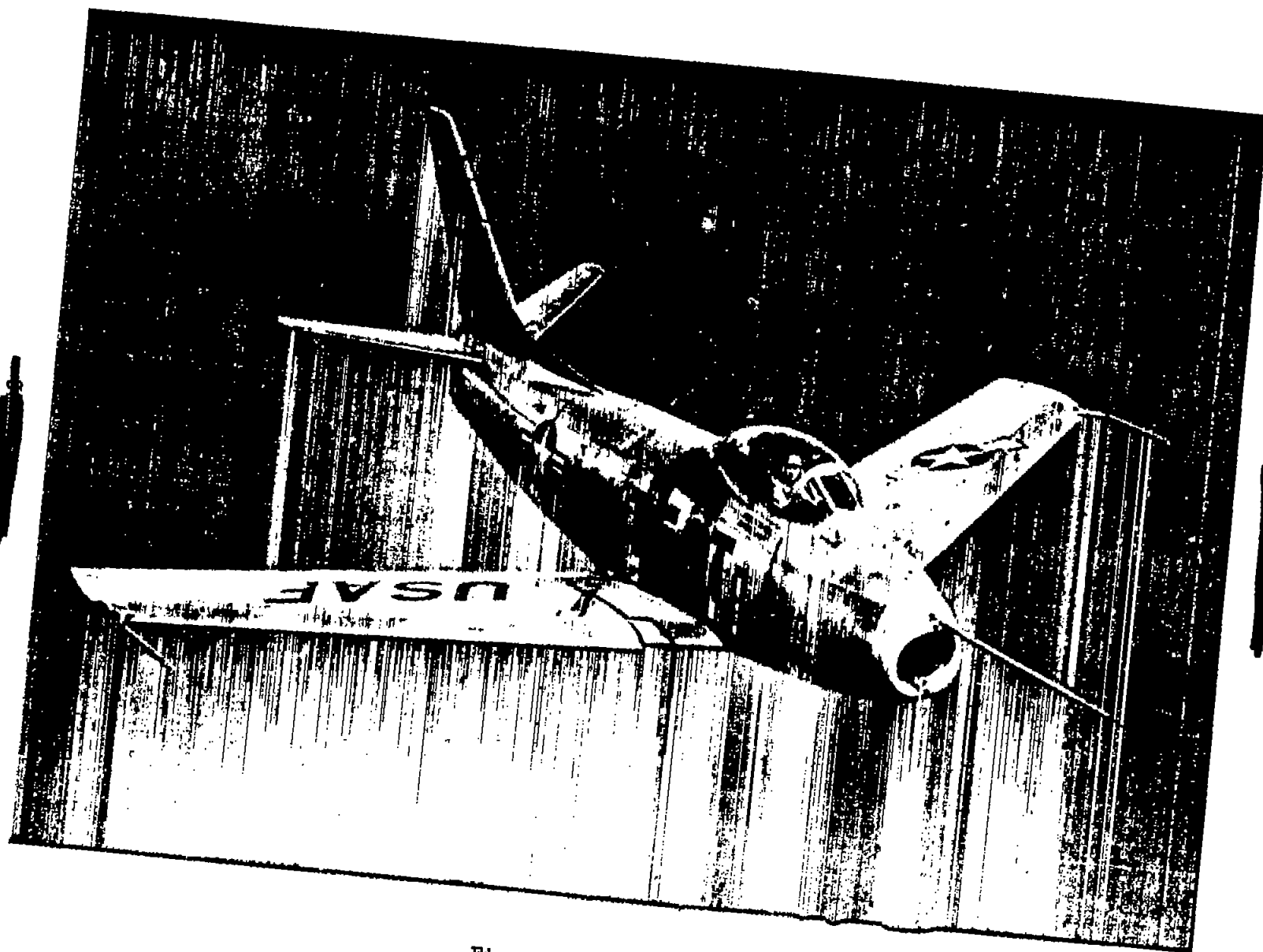
Figure 1.- Test airplane.

A-15019
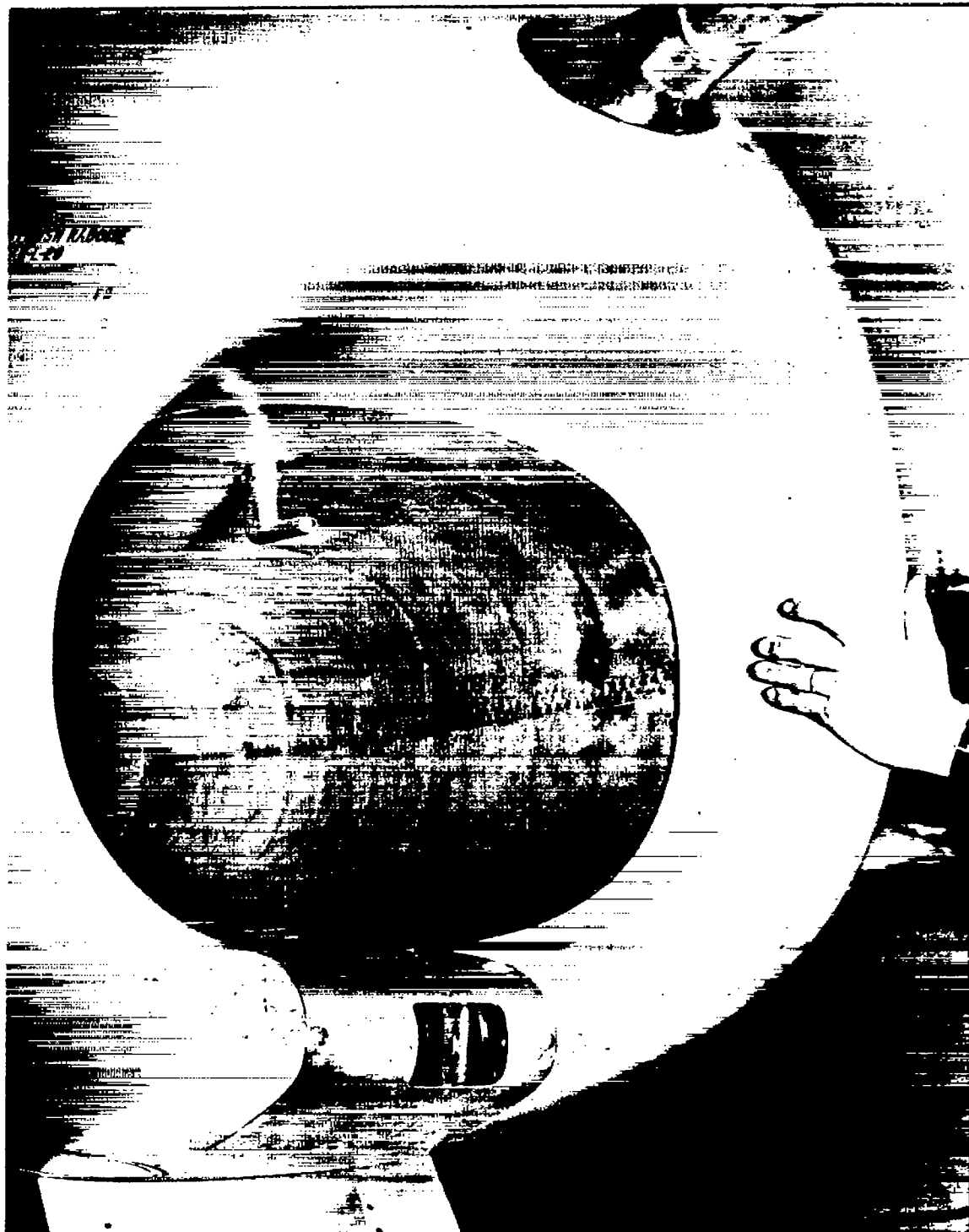
Figure 2.- Inlet detail.

A-14999

Station ① ②   ③

L.E. radius
1.375 in.

Compressor face

Scale = 1:40

Rake
location

Thrust line

Station, in.   15   40   60   80   100   120   140   160   185
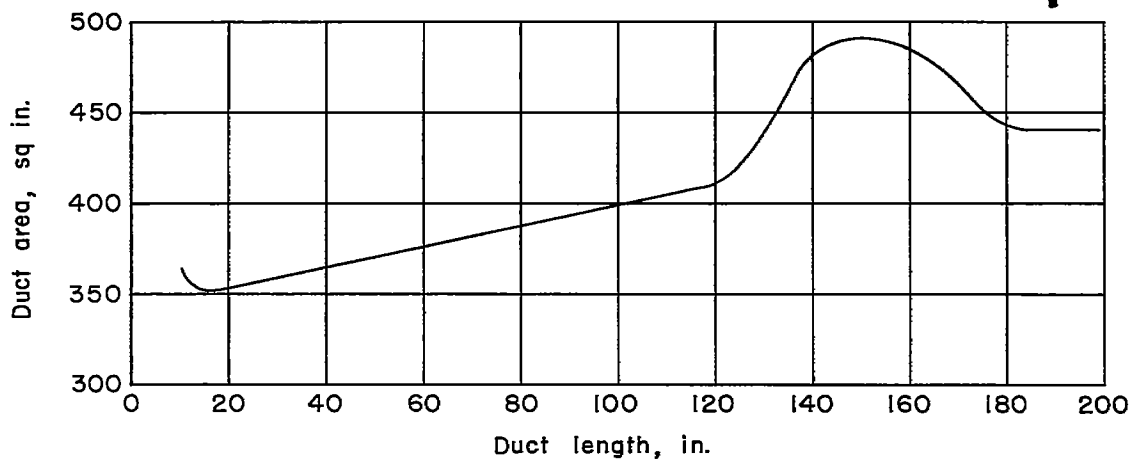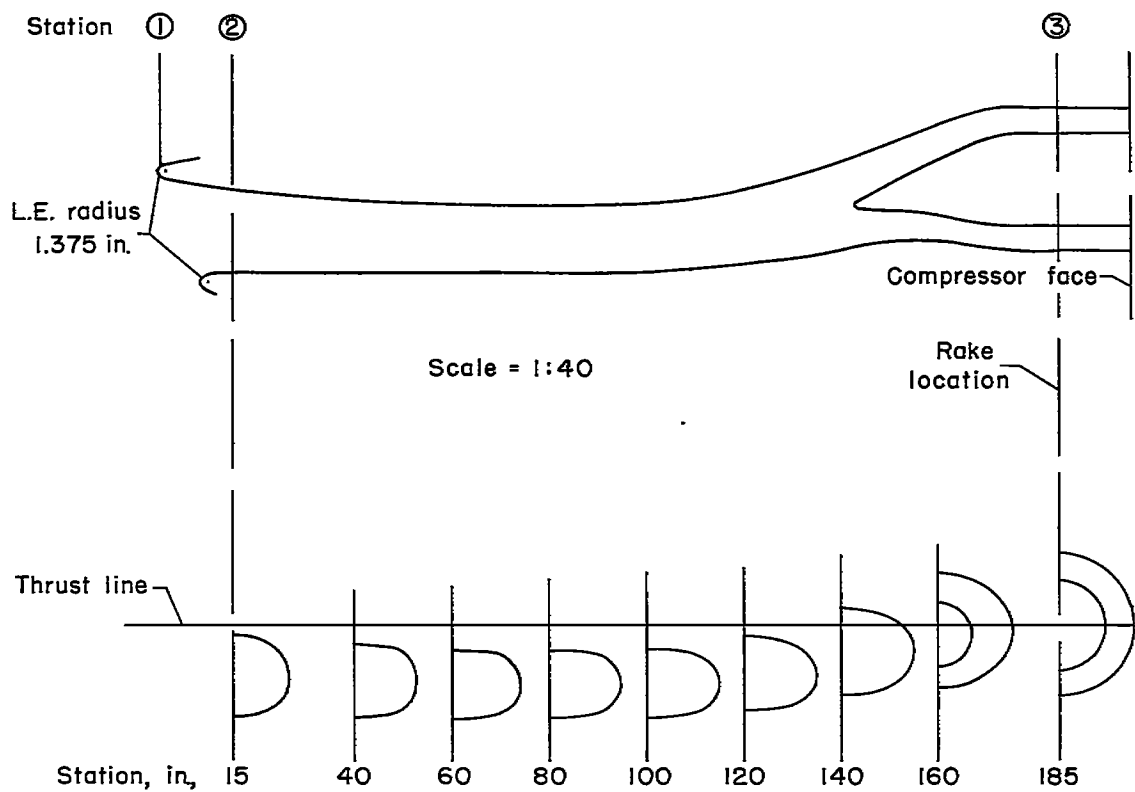
Figure 3.- Inlet detail and area distribution.

All dimensions in inches

30°

Outer wall

5.50

4.90

3.95

2.90

1.75

.50

Inner wall

(a) Rake detail.

69°

5.5

10.0

Inner
wall

Outer
wall

42°

69°

● Tube location

(b) Tube locations, looking aft.
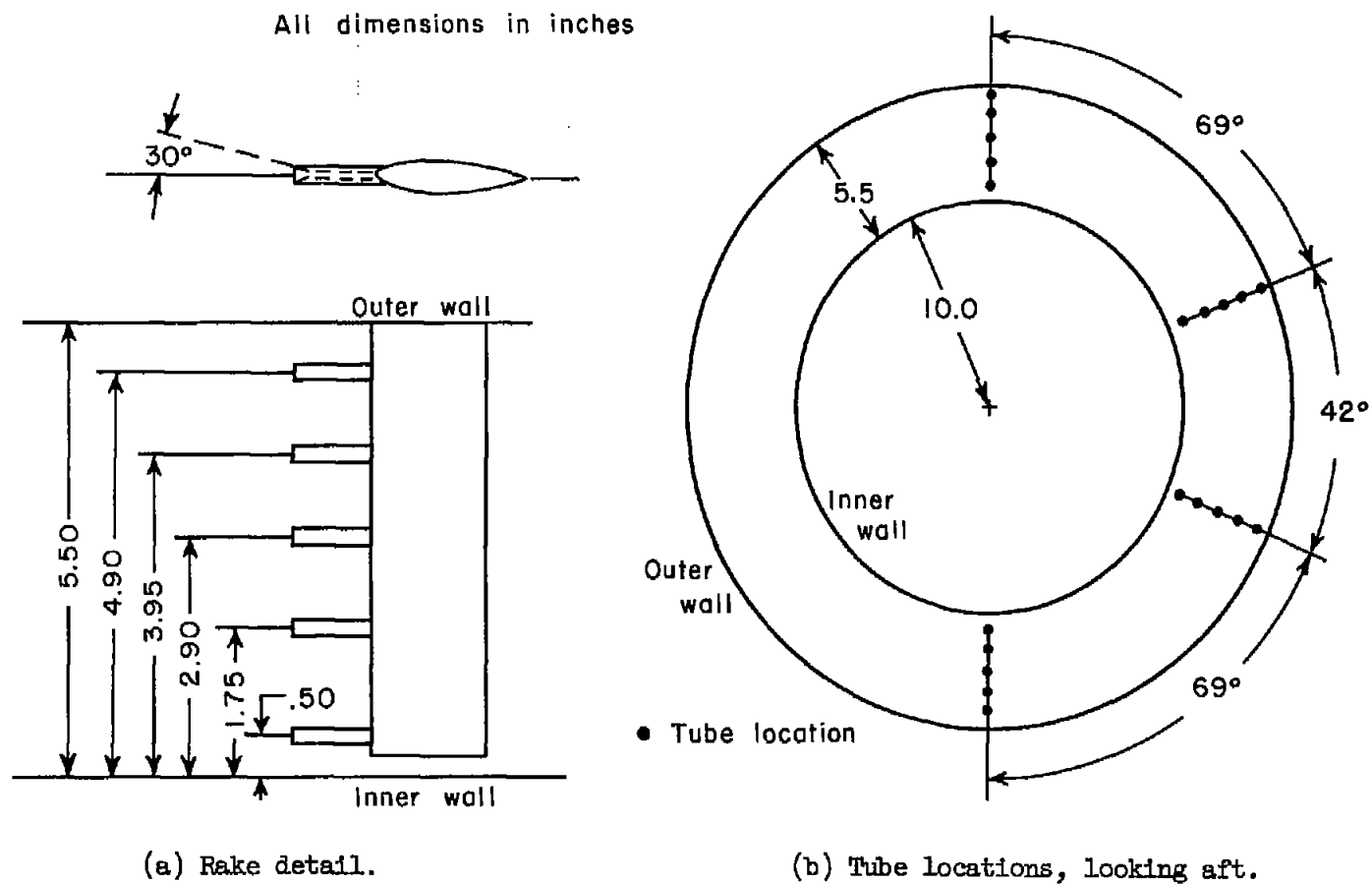
Figure 4.- Arrangement of total-pressure rakes.
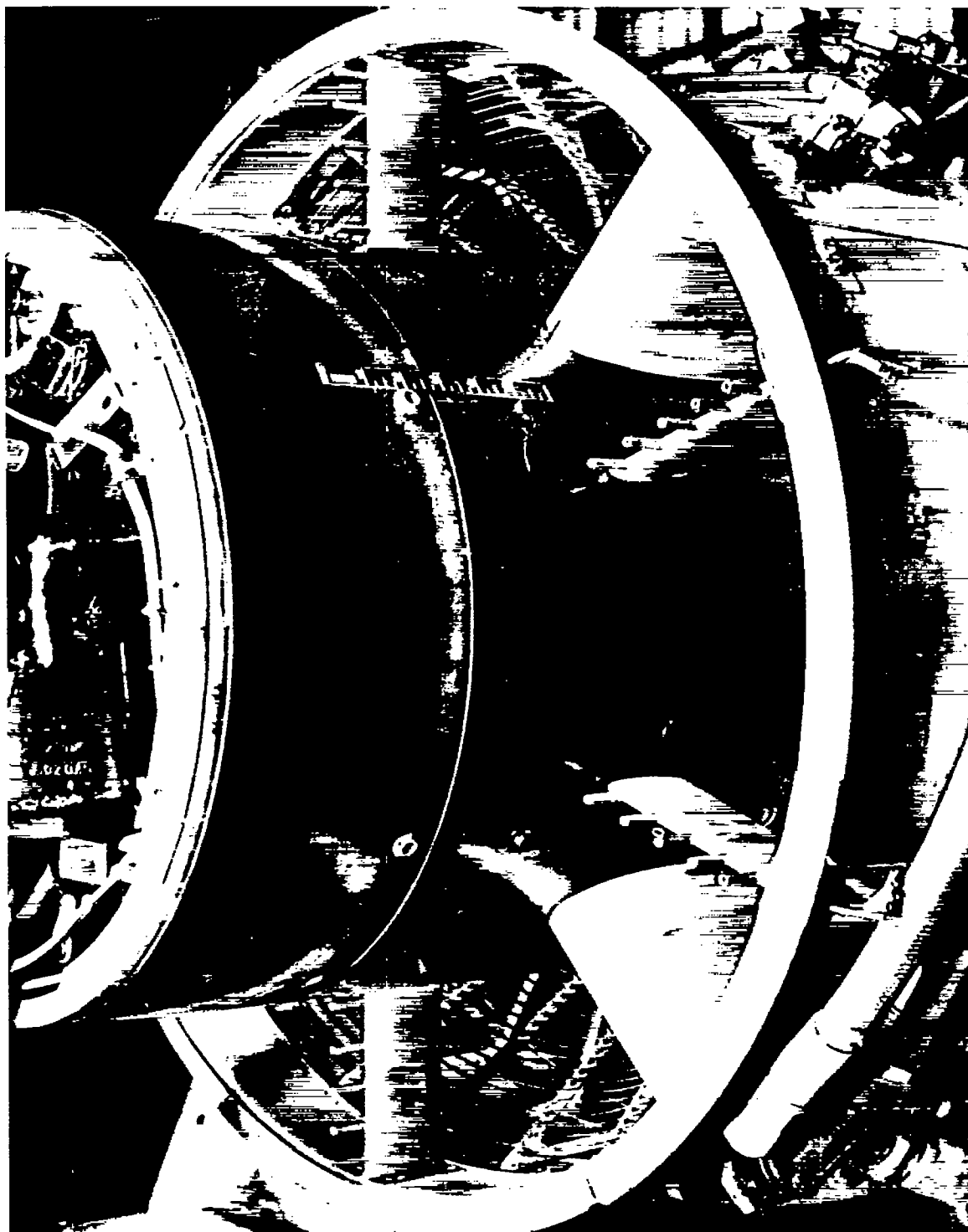
Figure 5.- Probe installations.

A-215'.
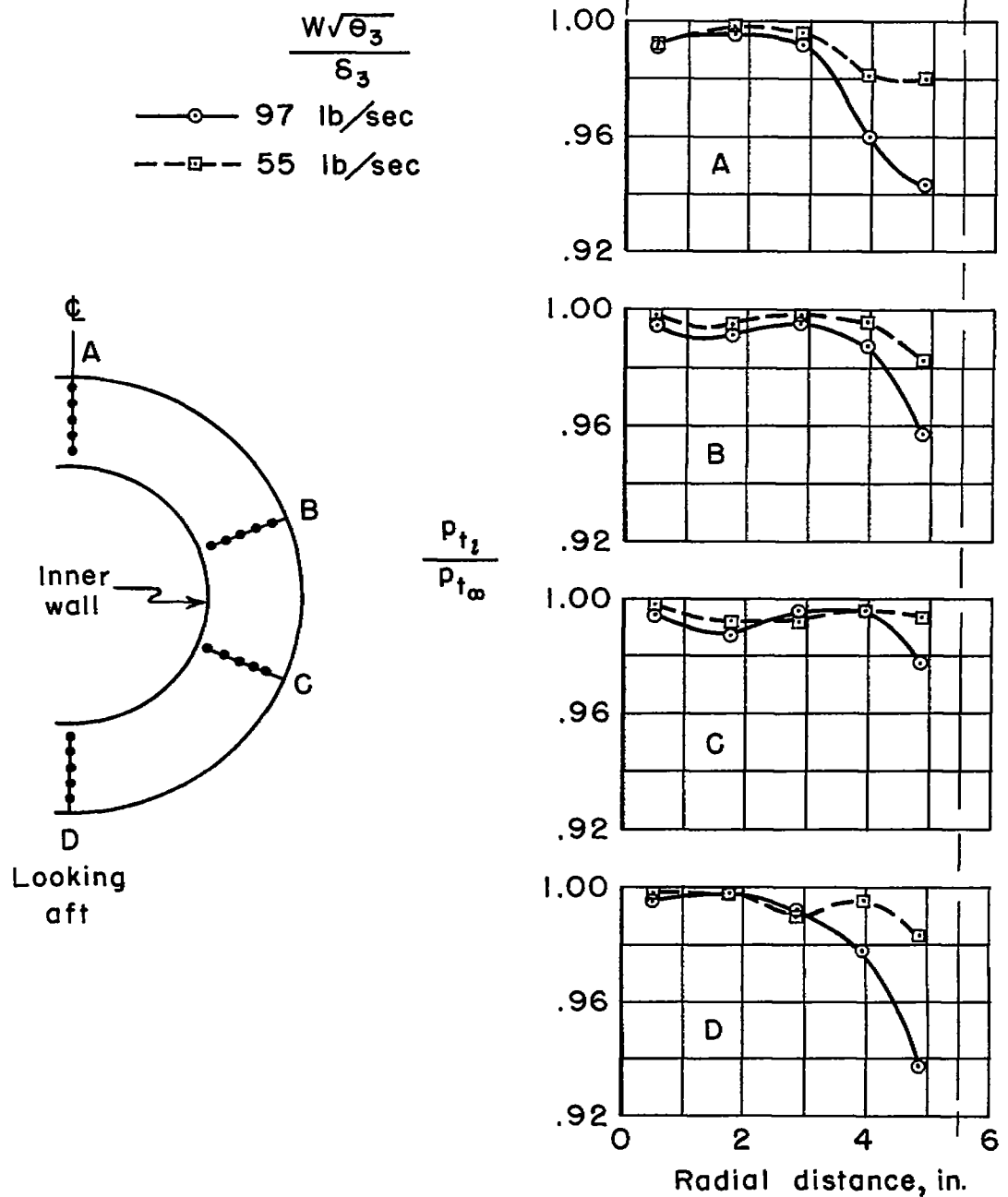
(a) $M_\infty = 0.78$, altitude = 35,000 feet, $\alpha = 3^\circ$

Figure 6.- Typical radial total-pressure profiles.
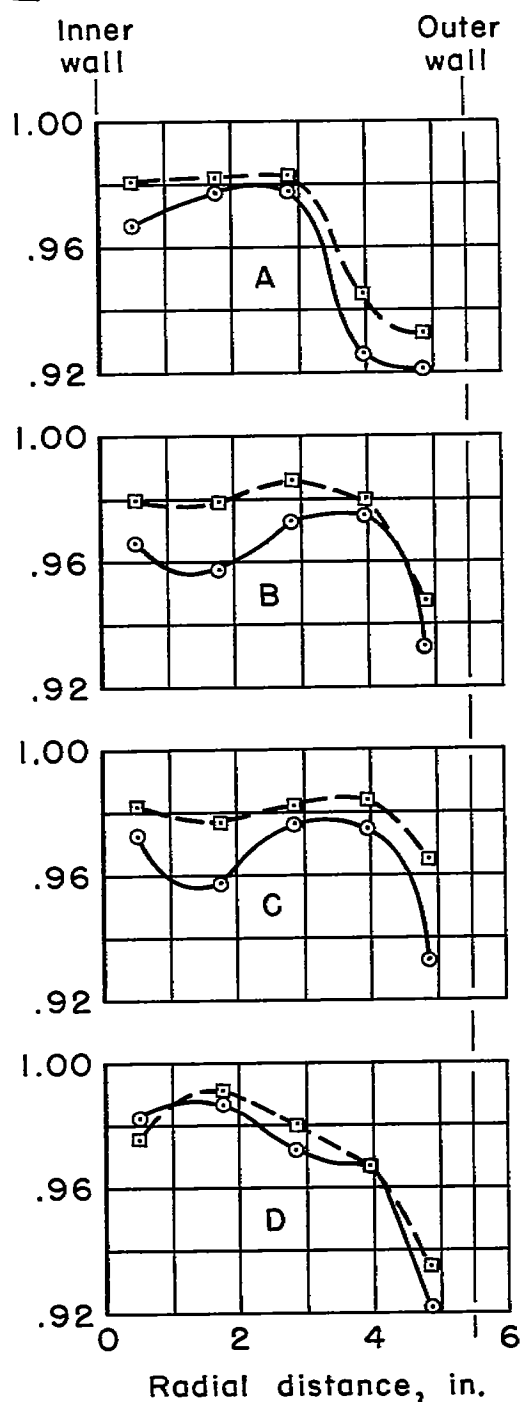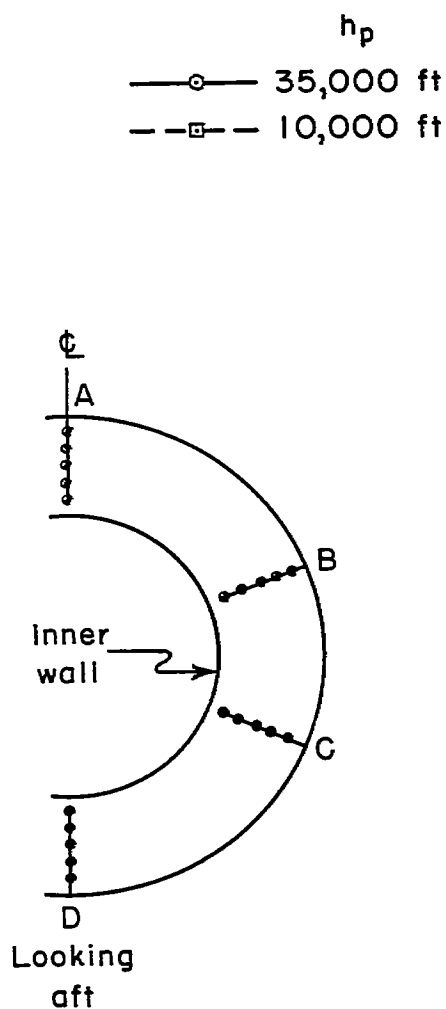
(b) $M_\infty = 0.60$, $\dfrac{W\sqrt{\theta_3}}{\delta_3} = 97$ lb/sec, $\alpha = 3^\circ$

Figure 6.- Continued.
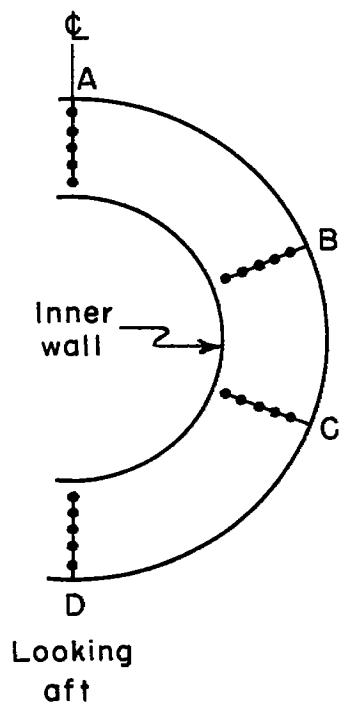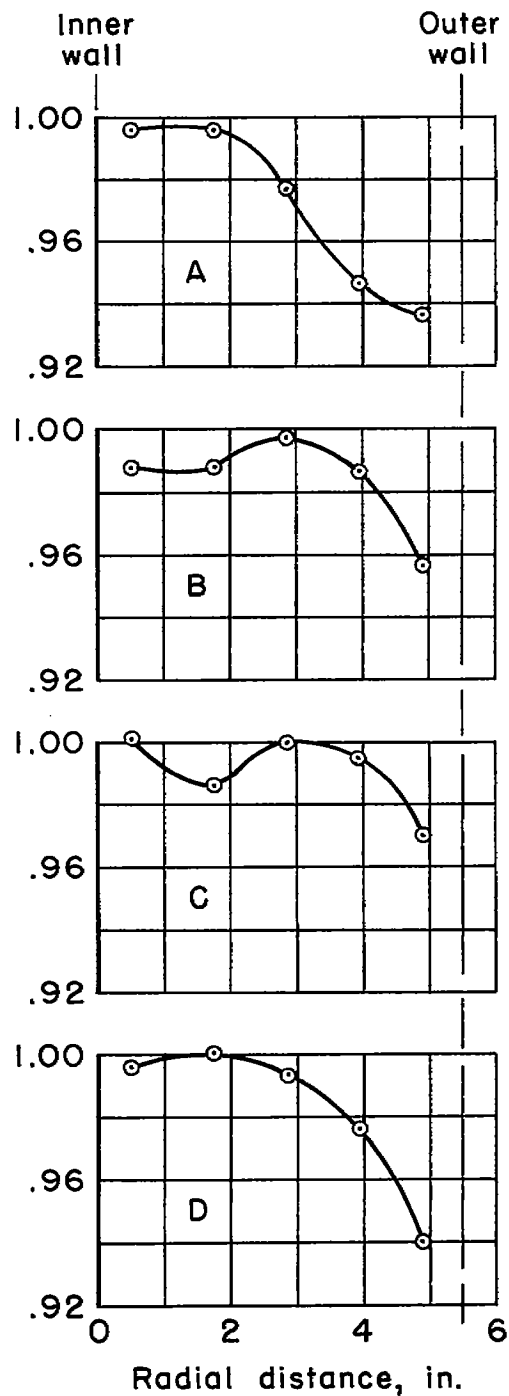
(c) $M_\infty = 1.03$, altitude = 35,000 feet, $\alpha = 3^\circ$, $\dfrac{W\sqrt{\theta_3}}{\delta_3} = 97$ lb/sec

Figure 6.- Continued.
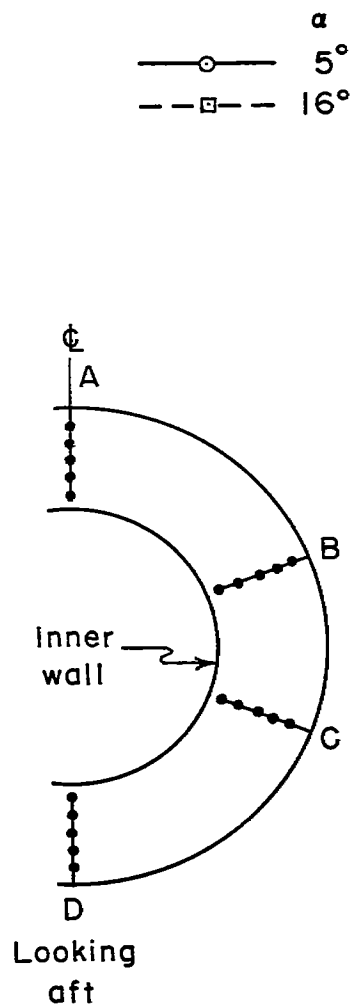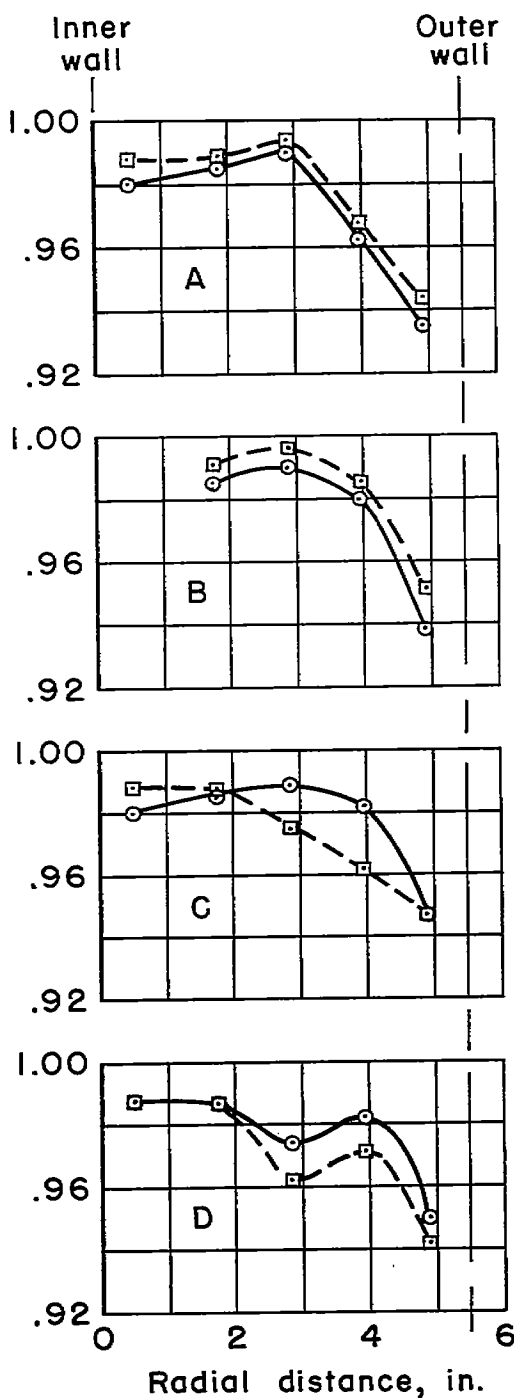
(d) $M_\infty \cong 0.30$, altitude = 25,000 feet, $\dfrac{W\sqrt{\theta_3}}{\delta_3} = 97$ lb/sec

Figure 6.- Concluded.
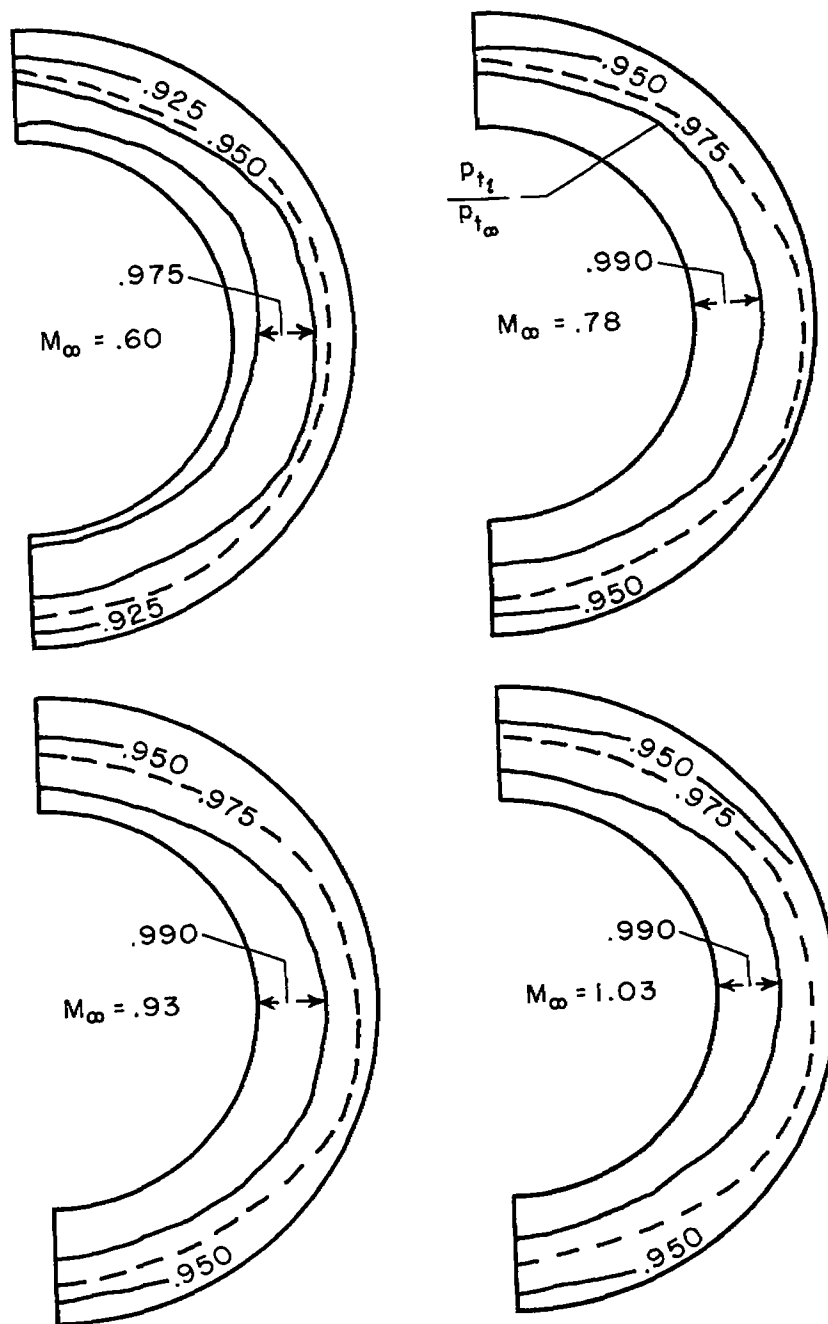
(a) $\dfrac{W\sqrt{\theta_3}}{\delta_3} = 97$ lb/sec, altitude = 25,000 feet, $\alpha = 3^{\circ}$

Figure 7.- Total-pressure contours at the compressor face; view looking aft.

$\frac{p_{t_l}}{p_{t_\infty}}$

.975

.990

$\alpha = 8°$

$\frac{W\sqrt{\Theta_3}}{\delta_3} = 80$ lb/sec

.975

.990

$\alpha = 16°$

$\frac{W\sqrt{\Theta_3}}{\delta_3} = 80$ lb/sec

.975 .950

.990

$\alpha = 8°$

$\frac{W\sqrt{\Theta_3}}{\delta_3} = 97$ lb/sec

.975 .950

.990

$\alpha = 16°$

$\frac{W\sqrt{\Theta_3}}{\delta_3} = 97$ lb/sec
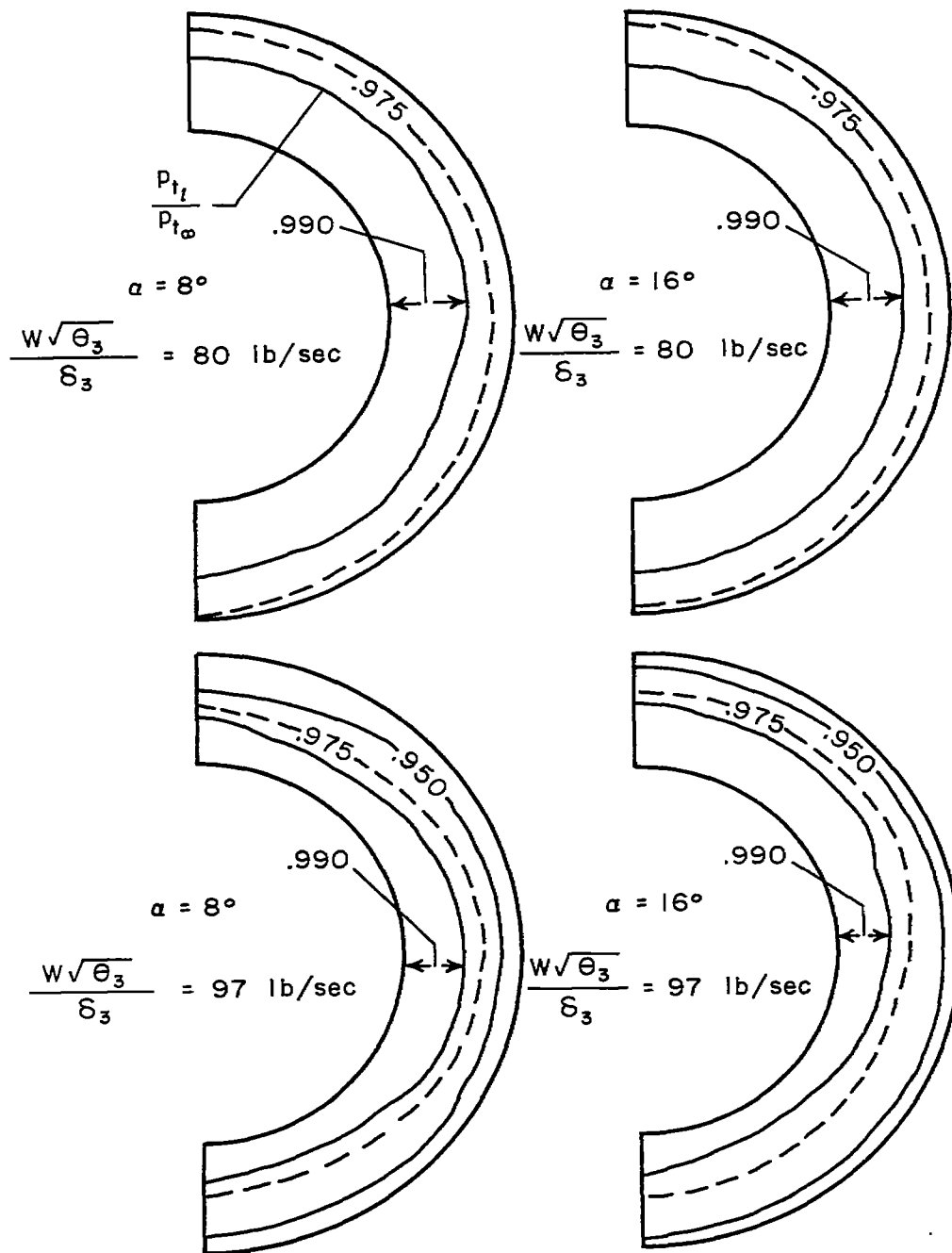
(b) $M_\infty \cong 0.30$, altitude = 25,000 feet

Figure 7.- Concluded.
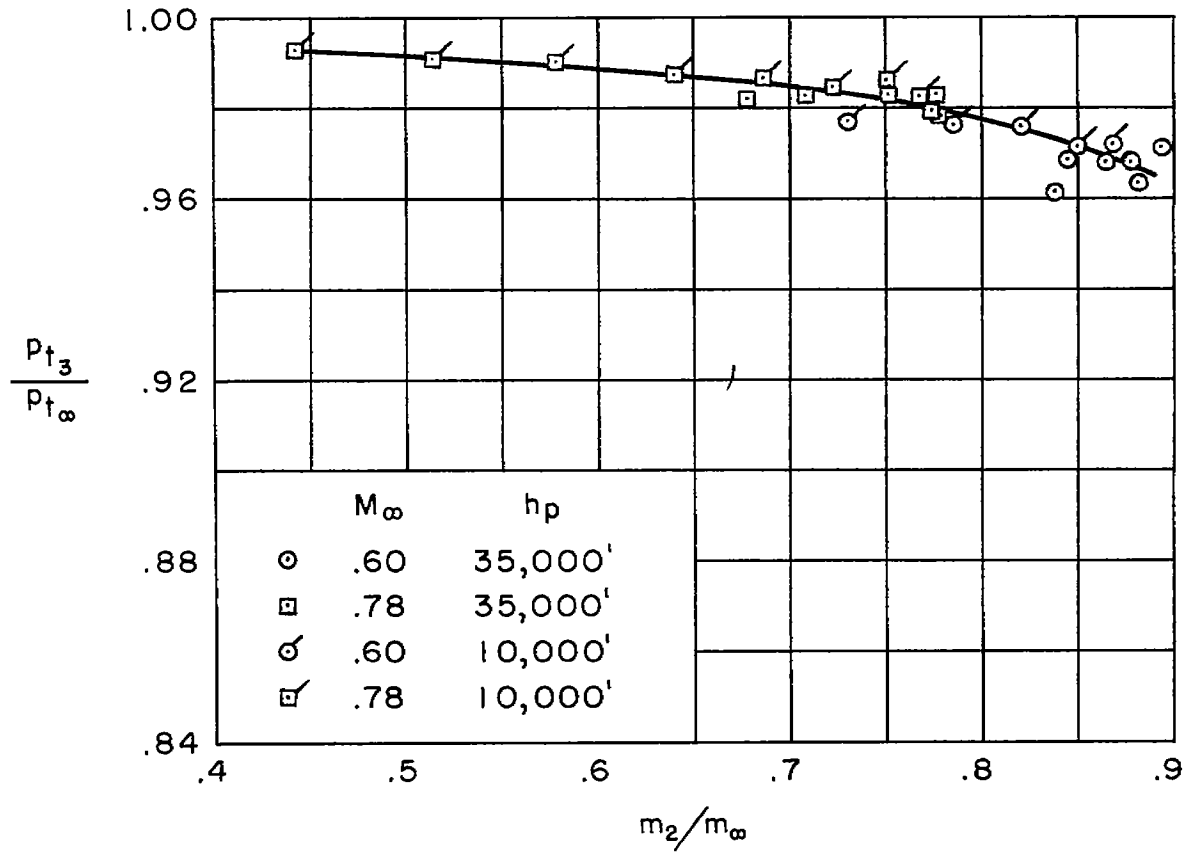
Figure 8.- Variation of average pressure recovery with mass-flow ratio; $\alpha = 3^{\circ}$.
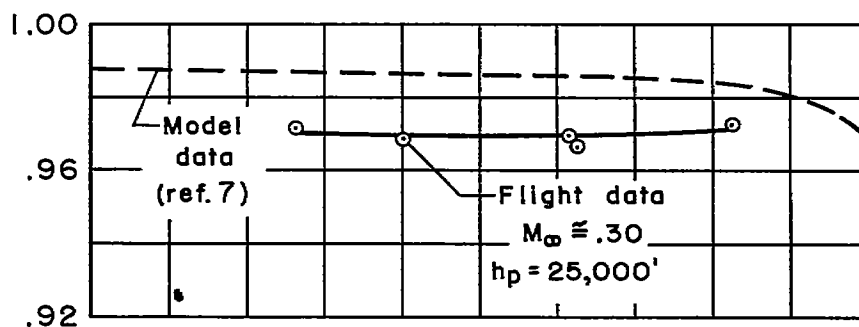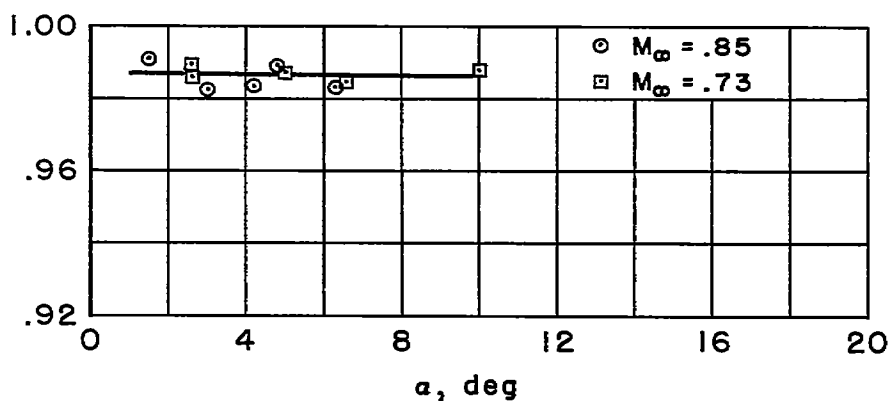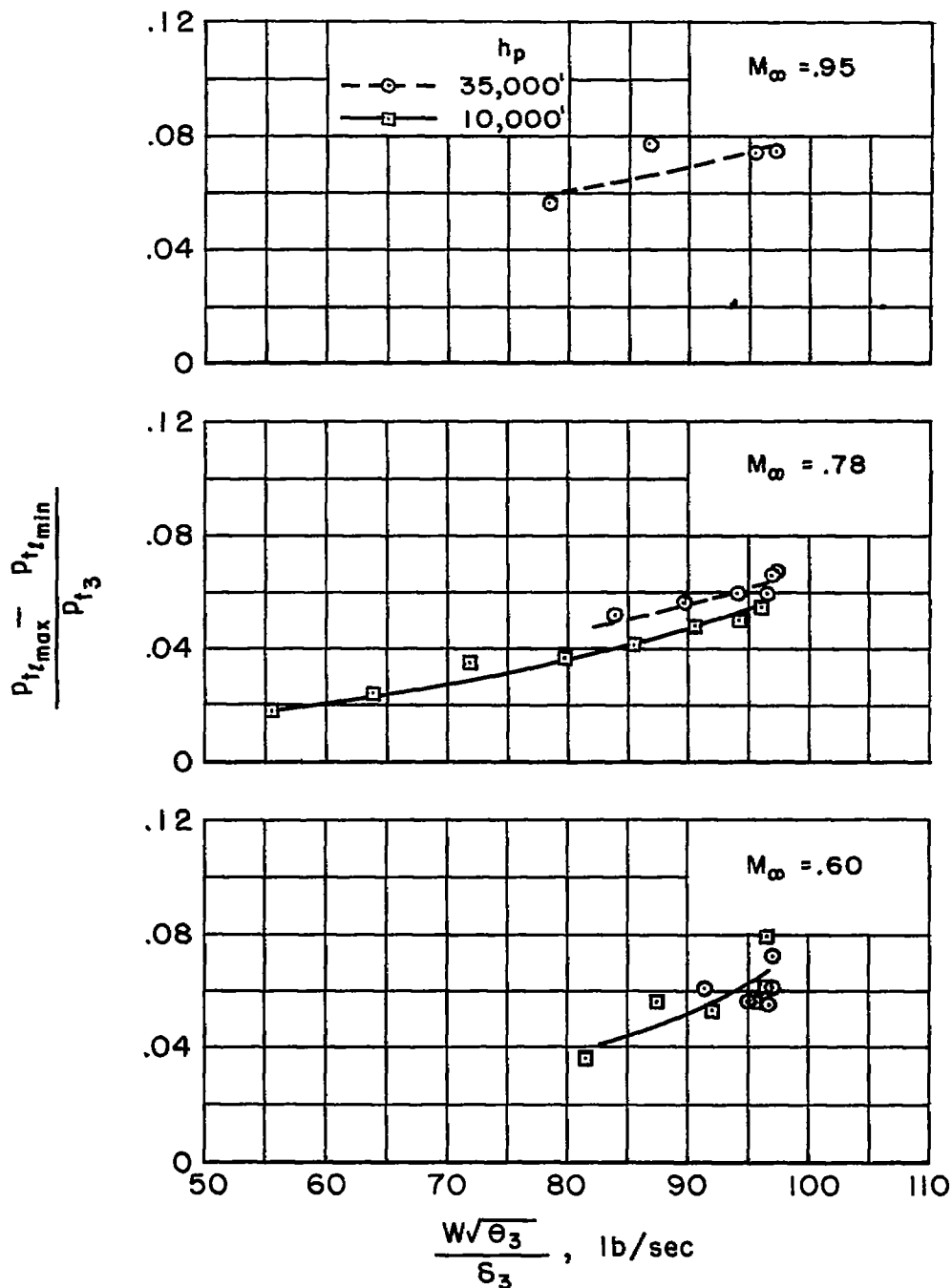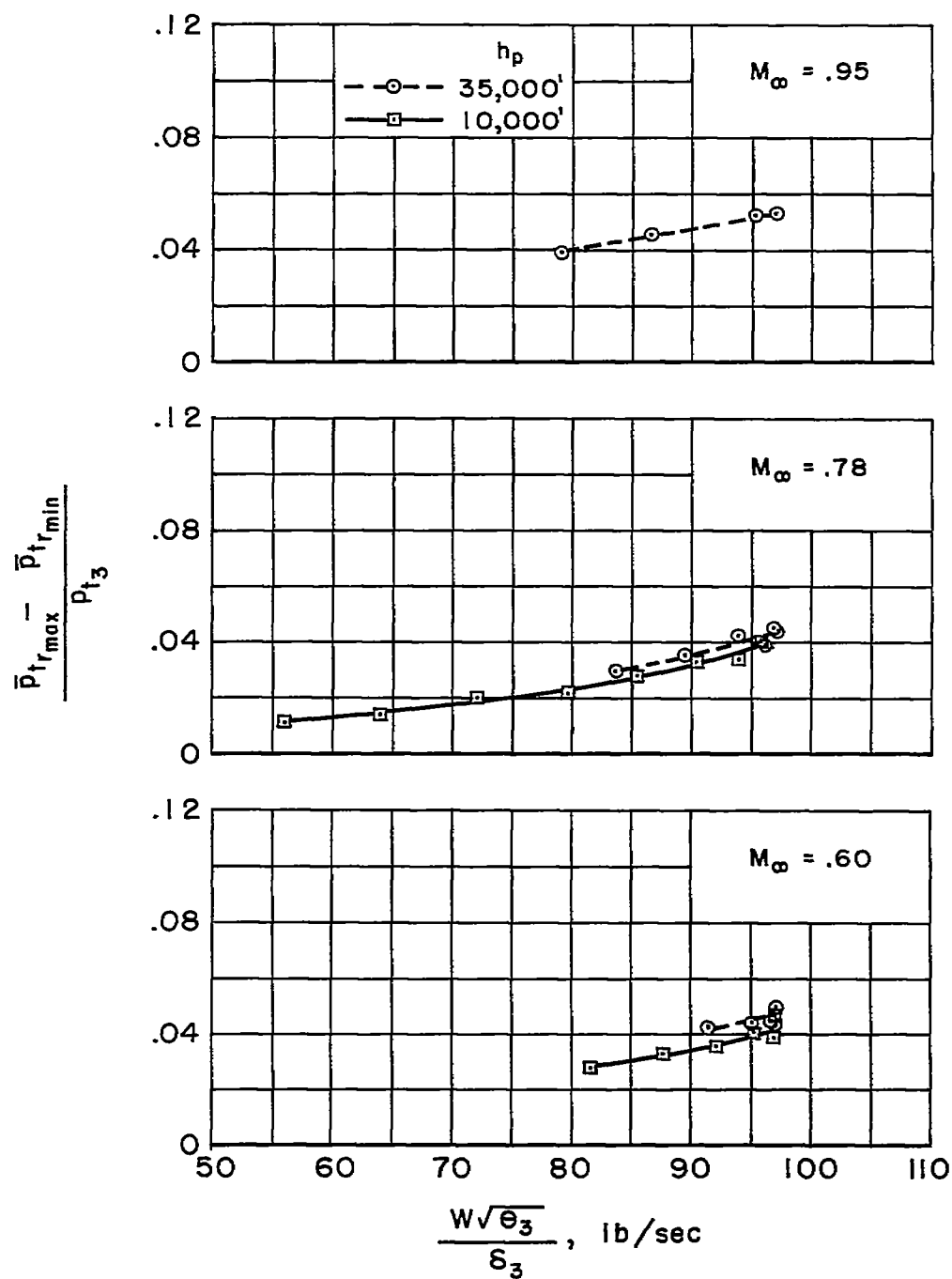
(a) $m_2/m_\infty = 2.1$
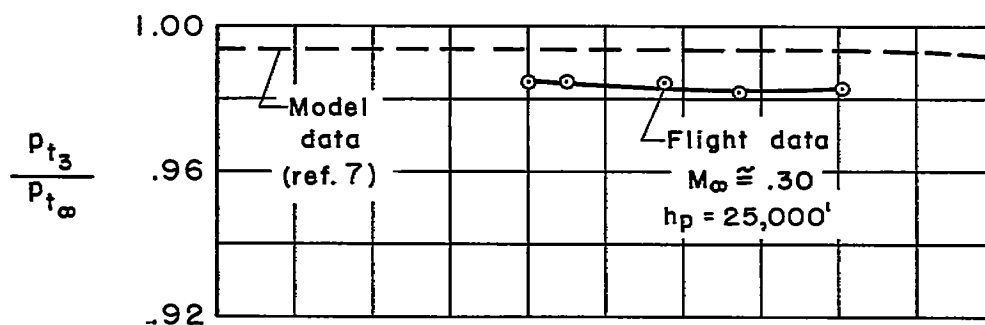
(b) $m_2/m_\infty = 1.8$

(c) $m_2/m_\infty = 0.7$, altitude = 35,000 feet

Figure 9.- Variation of average pressure recovery with angle of attack.
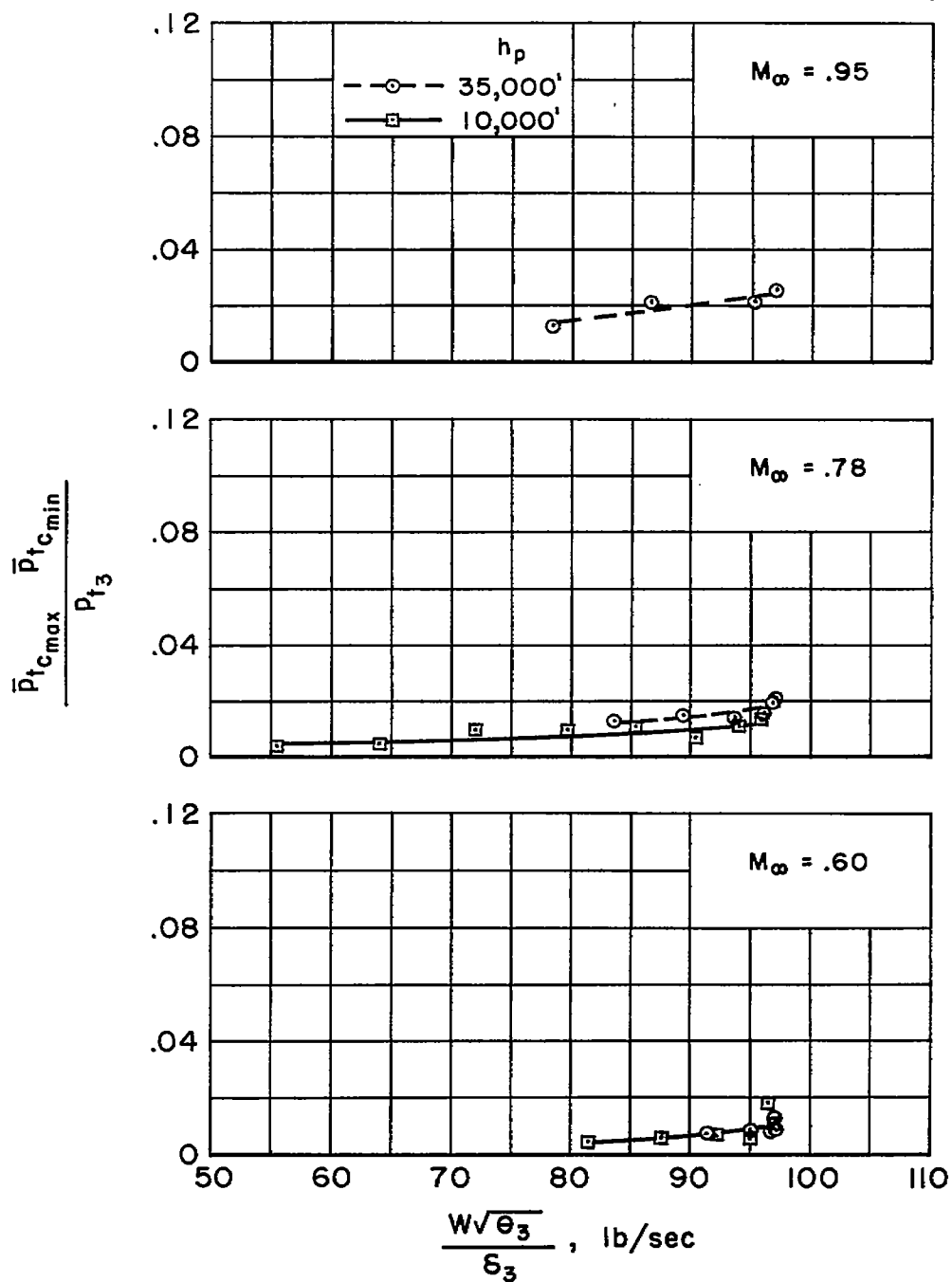
(a) Point total-pressure distortion.

Figure 10.- Variation of total-pressure distortion with corrected air flow; α = 3°.

(b) Average radial total-pressure distortion.

Figure 10.- Continued.

(c) Average circumferential total-pressure distortion.
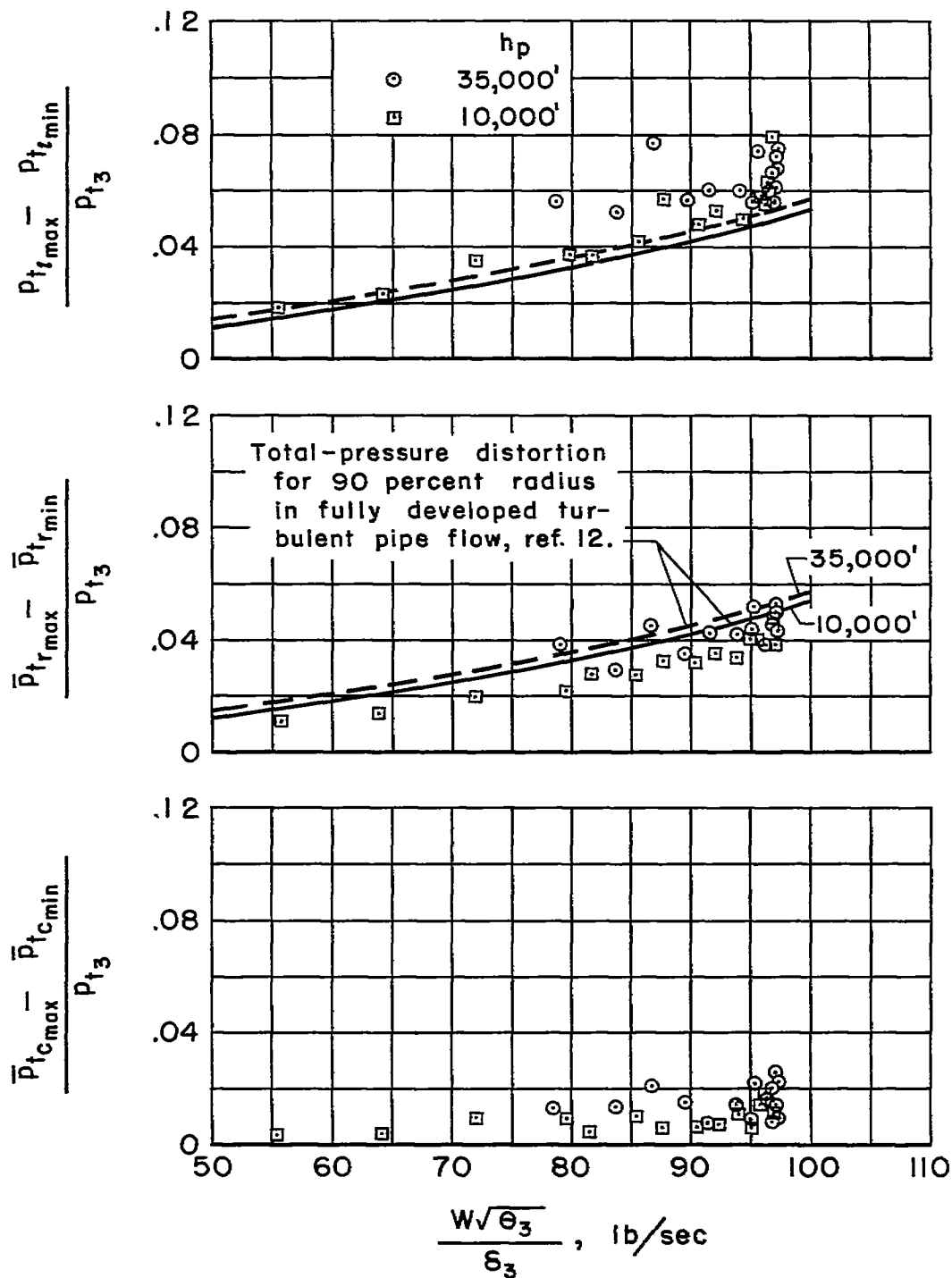
Figure 10.- Concluded.

Figure 11.- Variation of total-pressure distortion with corrected air
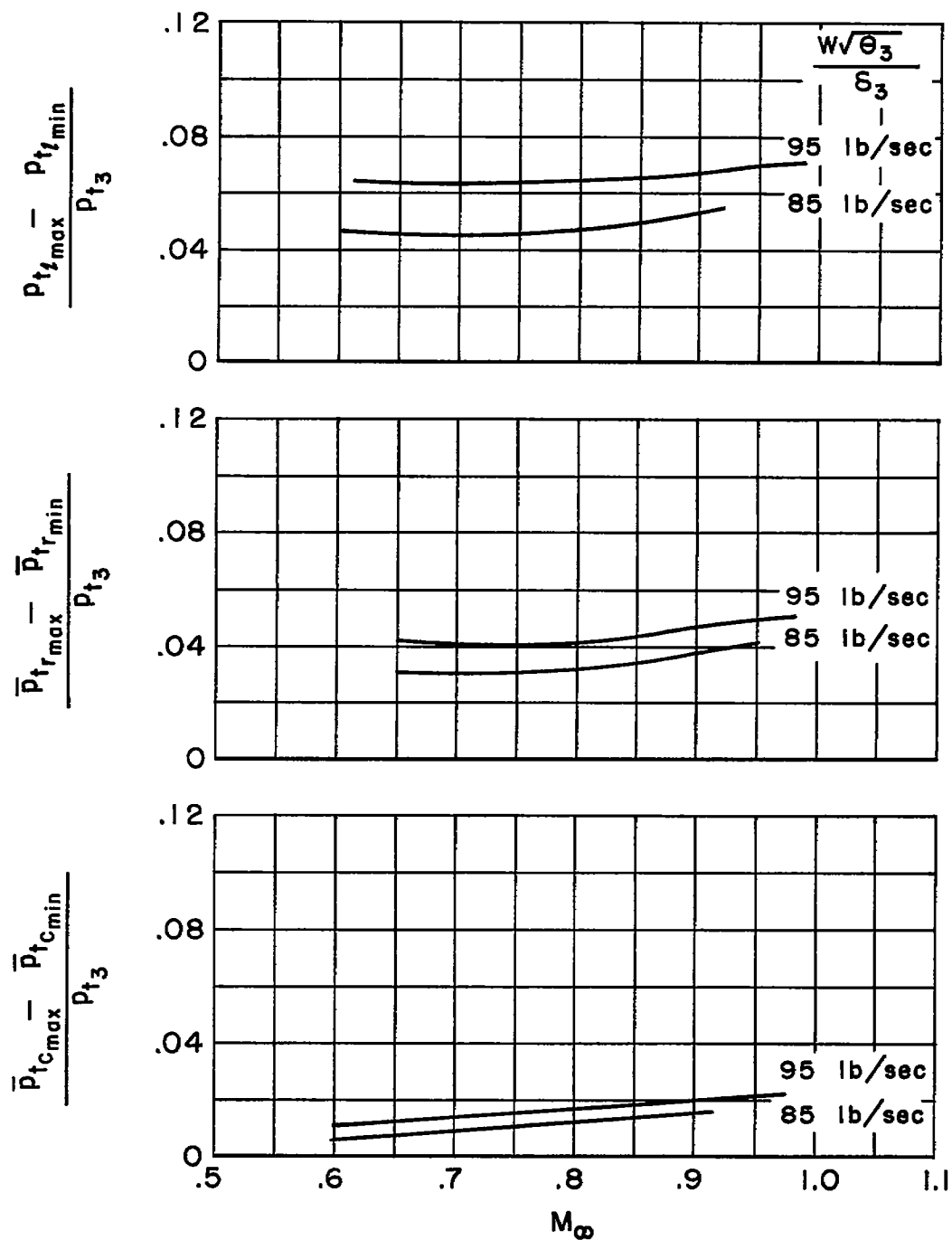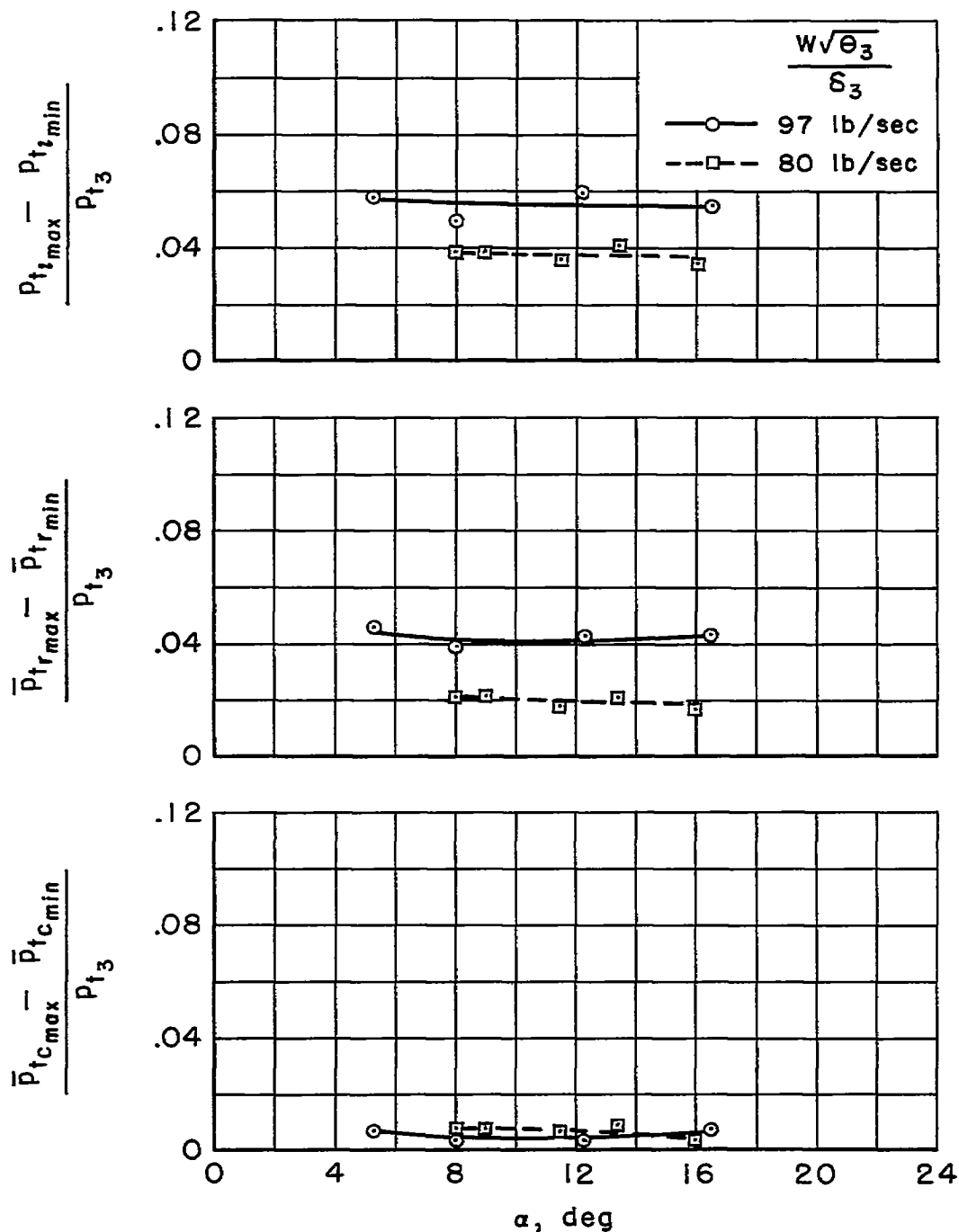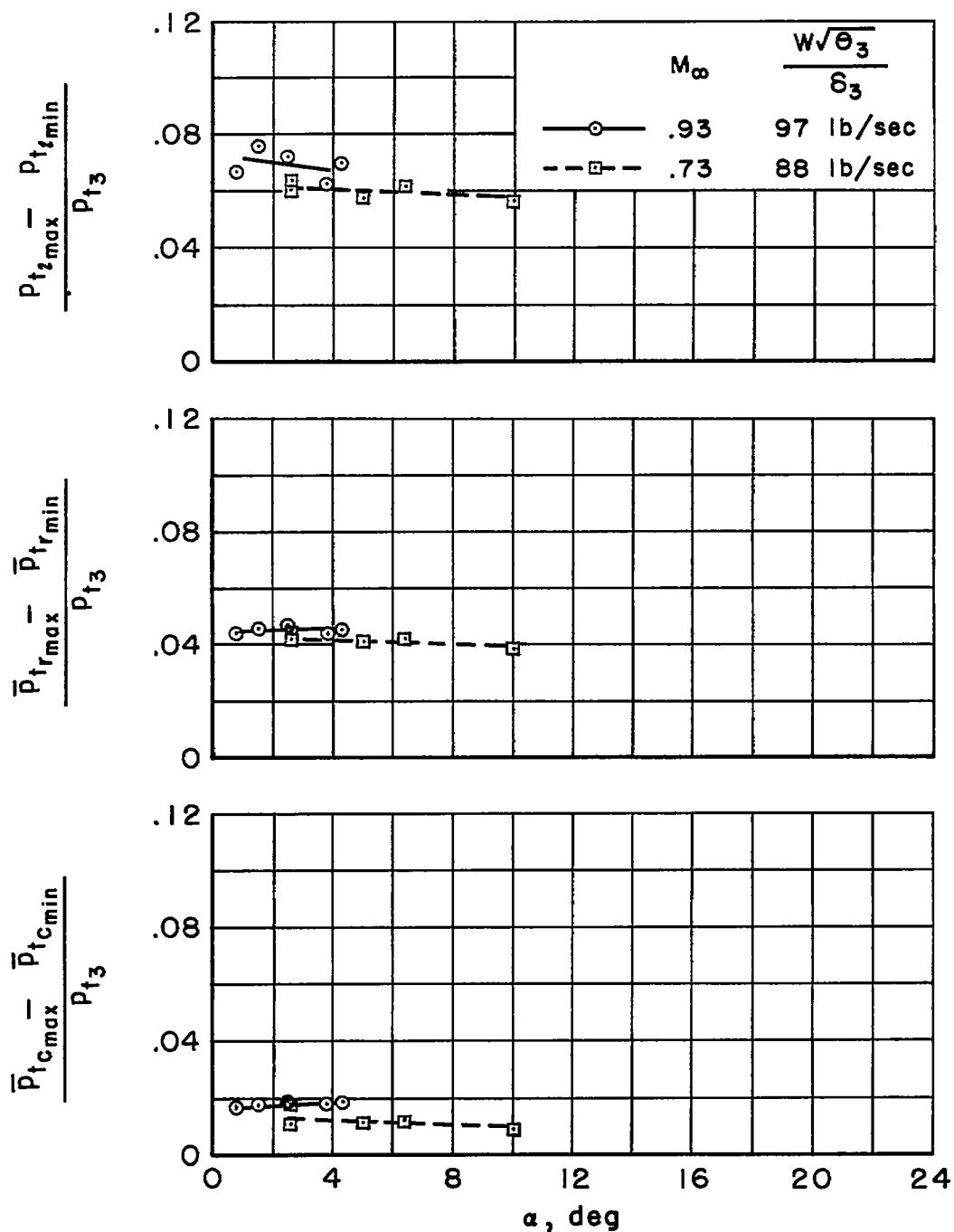flow; pipe cross-sectional area, 440 square inches.

Figure 12.- Variation of total-pressure distortion with Mach number; altitude = 35,000 feet, $\alpha = 3^{\circ}$.

(a) $M_\infty \cong 0.30$, altitude = 25,000 feet

Figure 13.- Variation of total-pressure distortion with angle of attack.

(b) $M_\infty = 0.93$ and 0.73, altitude = 35,000 feet

Figure 13.- Concluded.

NOTES: (1) Reynolds number is based on the diameter
of a circle with the same area as that
of the capture area of the inlet.

(2) The symbol * denotes the occurrence of
buzz.

Report and facility	Description			Test parameters				Test data				Performance		Remarks
	Configuration	Number of oblique shocks	Type of boundary-layer control	Free-stream Mach number, M	Reynolds number × 10⁻⁶	Angle of attack, deg, α	Angle of yaw, deg	Drag	Inlet-flow profile	Discharge-flow profile	Flow picture	Maximum total-pressure recovery	Mass-flow ratio	
Conf. RM A58B07 Ames Flight Research Branch	Compressor face — Measuring station — Full-Scale Aircraft Inlet		None	0.30 / 0.60 to 1.03	2.2 / 3.0 to 10.0	5 to 16 / 1 to 10	0 / 0					0.985 / 0.990	1.8 ~ 2.1 / 0.45 ~ 0.90	A maximum distortion of 8% was obtained from point measurements and maximum values of average radial and circumferential distortion were 5 and 2.5%, respectively. Effects of α, M, and inlet air flow were studied.
Conf. RM A58B07 Ames Flight Research Branch	Compressor face — Measuring station — Full-Scale Aircraft Inlet		None	0.30 / 0.60 to 1.03	2.2 / 3.0 to 10.0	5 to 16 / 1 to 10	0 / 0					0.985 / 0.990	1.8 ~ 2.1 / 0.45 ~ 0.90	A maximum distortion of 8% was obtained from point measurements and maximum values of average radial and circumferential distortion were 5 and 2.5%, respectively. Effects of α, M, and inlet air flow were studied.
Conf. RM A58B07 Ames Flight Research Branch	Compressor face — Measuring station — Full-Scale Aircraft Inlet		None	0.30 / 0.60 to 1.03	2.2 / 3.0 to 10.0	5 to 16 / 1 to 10	0 / 0					0.985 / 0.990	1.8 ~ 2.1 / 0.45 ~ 0.90	A maximum distortion of 8% was obtained from point measurements and maximum values of average radial and circumferential distortion were 5 and 2.5%, respectively. Effects of α, M, and inlet air flow were studied.
Conf. RM A58B07 Ames Flight Research Branch	Compressor face — Measuring station — Full-Scale Aircraft Inlet		None	0.30 / 0.60 to 1.03	2.2 / 3.0 to 10.0	5 to 16 / 1 to 10	0 / 0					0.985 / 0.990	1.8 ~ 2.1 / 0.45 ~ 0.90	A maximum distortion of 8% was obtained from point measurements and maximum values of average radial and circumferential distortion were 5 and 2.5%, respectively. Effects of α, M, and inlet air flow were studied.

Bibliography

These strips are provided for the convenience of the reader and can be removed from this report to
compile a bibliography of NACA inlet reports. This page is being
added only to inlet reports and is on a trial basis.